Density functional theory for hard-sphere mixtures: the White-Bear version Mark II

Hendrik Hansen-Goos†‡and Roland Roth †‡

† Max-Planck-Institut für Metallforschung - Heisenbergstr. 3, 70569 Stuttgart, Germany

‡ ITAP, Universität Stuttgart - Pfaffenwaldring 57, 70569 Stuttgart, Germany

E-mail: hhansen@fluids.mpi-stuttgart.mpg.de

Abstract. In the spirit of the White-Bear version of fundamental measure theory we derive a new density functional for hard-sphere mixtures which is based on a recent mixture extension of the Carnahan-Starling equation of state. In addition to the capability to predict inhomogeneous density distributions very accurately, like the original White-Bear version, the new functional improves upon consistency with an exact scaled-particle theory relation in the case of the pure fluid. We examine consistency in detail within the context of morphological thermodynamics. Interestingly, for the pure fluid the degree of consistency of the new version is not only higher than for the original White-Bear version but also higher than for Rosenfeld's original fundamental measure theory.

1. Introduction

In the mid 1970s, density functional theory, which was originally formulated for quantum systems, has been extended to systems that follow classical statistical mechanics [1]. Since then, density functional theory of classical systems (DFT) has developed to an indispensable tool for the study of inhomogeneous systems such as crystals, fluids in confined geometries [2], liquid-vapor interfaces and wetting and drying on substrates (for a recent review see [3]). DFT is based on the fact that there exists a functional $\Omega[\rho]$ of the spatially varying particle number density $\rho(\mathbf{r})$ which possesses two properties: (i) it is minimized by the equilibrium density $\rho_0(\mathbf{r})$, and (ii) the minimum value $\Omega[\rho_0]$ equals the grand potential Ω of the system. These properties give rise to the variational principle $\delta\Omega[\rho]/\delta\rho \equiv 0$ for $\rho(\mathbf{r}) = \rho_0(\mathbf{r})$.

One can decompose $\Omega[\rho]$ as

$$\Omega[\rho] = \mathcal{F}[\rho] + \int \mathrm{d}\mathbf{r}\, \rho(\mathbf{r})(V_{\mathrm{ext}}(\mathbf{r}) - \mu)\,, \tag{1}$$

where μ is the chemical potential, $V_{\mathrm{ext}}(\mathbf{r})$ the external potential acting on the particles and $\mathcal{F}[\rho]$ is a unique functional corresponding to the intrinsic Helmholtz free energy of the system in equilibrium.

In principle, Eq. (1) with the variational principle constitutes an excellent tool for (numerical) calculations of $\rho_0(\mathbf{r})$ and hence the grand potential $\Omega[\rho_0(\mathbf{r})]$ in arbitrary external potentials. Unfortunately, for many systems of interest, only more or less crude approximations for $\mathcal{F}[\rho]$ are known. The expression for the ideal gas, however, is known exactly

$$\beta\mathcal{F}_{\mathrm{id}}[\rho] = \int \mathrm{d}\mathbf{r}\, \rho(\mathbf{r}) \left(\ln(\Lambda^3\rho(\mathbf{r})) - 1\right) , \tag{2}$$

where Λ is the thermal wavelength of the particles and $\beta = 1/(k_{\mathrm{B}}T)$ with Boltzmann's constant k_{B} and the temperature T. The interactions among particles are described by the excess (over ideal gas) free energy $\mathcal{F}_{\mathrm{ex}}[\rho] = \mathcal{F}[\rho] - \mathcal{F}_{\mathrm{id}}[\rho]$ which for our purposes can be expressed as $\beta\mathcal{F}_{\mathrm{ex}} = \int \mathrm{d}\mathbf{r}\Phi(\mathbf{r})$, where the excess free energy density $\Phi(\mathbf{r})$ is a functional of $\rho(\mathbf{r})$.

In this work we direct our attention to mixtures of hard-spheres. For these systems, the exact expression for $\mathcal{F}_{\mathrm{ex}}$ is unknown but a number of approximations can be found in the literature [4]. The interest in the hard-sphere system is manifold. The hard-sphere system serves as a reference system for fluids with short-ranged repulsion and additional attractive interactions among particles. The attractive part of the potential is usually treated perturbatively [5]. Furthermore, colloidal suspensions with quasi hard-sphere interactions can be realized experimentally (see, e.g. [6]) which provides a test ground for predictions from the field of the purely entropically driven hard-sphere systems, like entropic forces [7], asymptotic decay of correlation functions in mixtures [8, 9] etc..

A very successful class of excess free energy functionals is formulated within the framework of fundamental measure theory (FMT) introduced by Rosenfeld [10]. While the original FMT has the Percus-Yevick (PY) equation of state as an output, later, with the setup of the White-Bear version of FMT [11, 12], the more accurate Carnahan-Starling (CS) equation of state was incorporated into FMT. The resulting gain in precision in the structure of inhomogeneous density distribution [11, 12, 13] and in thermodynamics, however, has to be paid for with a slight inconsistency appearing on the level of the pressure [11]: the pressure in the hard-sphere fluid obtained from a scaled-particle theory equation differs slightly from the underlying bulk equation of state. The aim of this work is to build upon the White-Bear version of FMT, using a new mixture formulation of the CS equation of state [14], such that this inconsistency is resolved.

The paper is organized as follows. In Sec. 2 we review Rosenfeld's derivation of FMT. Section 3 is dedicated to the presentation of the White-Bear version of FMT and the derivation of the new version of FMT. In Sec. 4 we give a brief introduction to morphological thermodynamics of hard-sphere fluids and compare the performance of Rosenfeld's FMT and the original White-Bear version with that of the new functional. Section 5 contains our conclusion.

2. Fundamental measure theory

In a seminal paper in 1989, Rosenfeld set up FMT, allowing him to derive his successful free energy functional for the hard-sphere mixture [10]. We sketch his approach briefly in the following.

We consider a ν-component hard-sphere mixture with spatially varying particle number densities $\rho_i(\mathbf{r})$, $i = 1, \ldots, \nu$. From the theory of diagrammatic expansions [5] the excess free energy functional in the low-density limit is known exactly. One finds that the Mayer-f function, related to the pair interaction potential $V_{ij}(r)$ between the particles of species i and j by $f_{ij}(r) = \exp[-\beta V_{ij}(r)] - 1$, plays a central role. In the case of hard spheres, V_{ij} is either infinite if spheres overlap and zero otherwise. As a result the Mayer-f function obtains a purely geometrical meaning: $f_{ij}(r) = -\Theta(R_i + R_j - r)$ where R_i and R_j are the radii of the respective species and Θ is the Heaviside function.

Inspired by the exact excess free energy functional of the one-dimensional hard-rod mixture [15, 16], the key-idea of FMT is the deconvolution of the Mayer-f function $f_{ij}(r)$ into a sum of products with factors depending only on one of R_i and R_j. Rosenfeld's deconvolution reads

$$-f_{ij}(|\mathbf{r}_i - \mathbf{r}_j|) = \omega_0^i \otimes \omega_3^j + \omega_3^i \otimes \omega_0^j + \omega_1^i \otimes \omega_2^j + \omega_2^i \otimes \omega_1^j - \boldsymbol{\omega}_1^i \otimes \boldsymbol{\omega}_2^j - \boldsymbol{\omega}_2^i \otimes \boldsymbol{\omega}_1^j \quad (3)$$

with four scalar and two vectorial (weight) functions

$$\omega_3^i(\mathbf{r}) = \Theta(R_i - |\mathbf{r}|)\,, \quad \omega_2^i(\mathbf{r}) = \delta(R_i - |\mathbf{r}|)\,, \quad \boldsymbol{\omega}_2^i(\mathbf{r}) = \frac{\mathbf{r}}{|\mathbf{r}|}\,\delta(R_i - |\mathbf{r}|)\,, \quad (4)$$

and $\omega_1^i(\mathbf{r}) = \omega_2^i(\mathbf{r})/(4\pi R_i)$, $\omega_0^i(\mathbf{r}) = \omega_2^i(\mathbf{r})/(4\pi R_i^2)$, and $\boldsymbol{\omega}_1^i(\mathbf{r}) = \boldsymbol{\omega}_2^i(\mathbf{r})/(4\pi R_i)$. The convolution product $\otimes$ in Eq. (3) is defined by

$$\omega_\alpha^i \otimes \omega_\gamma^j = \int \mathrm{d}\mathbf{r}\, \omega_\alpha^i(\mathbf{r} - \mathbf{r}_i) \cdot \omega_\gamma^j(\mathbf{r} - \mathbf{r}_j)\,, \quad (5)$$

where the dot $\cdot$ stands for the usual product in the case of the scalar weight functions and for the scalar product in the case of the vectorial weight functions. Using the weight functions, one can define weighted densities

$$n_\alpha(\mathbf{r}) = \sum_{i=1}^{\nu} \int \mathrm{d}\mathbf{r}' \rho_i(\mathbf{r}') \omega_\alpha^i(\mathbf{r} - \mathbf{r}')\,. \quad (6)$$

The deconvolution, Eq. (3), can be used to express the exact low-density limit of the excess free energy functional:

$$\begin{aligned} \lim_{\rho_i \to 0} \beta\mathcal{F}^{\mathrm{ex}} &= -\frac{1}{2} \sum_{i,j=1}^{\nu} \int \mathrm{d}\mathbf{r}\mathrm{d}\mathbf{r}' \rho_i(\mathbf{r}) \rho_j(\mathbf{r}') f_{ij}(|\mathbf{r} - \mathbf{r}'|) \\ &= \int \mathrm{d}\mathbf{r} (n_0(\mathbf{r}) n_3(\mathbf{r}) + n_1(\mathbf{r}) n_2(\mathbf{r}) - \mathbf{n}_1(\mathbf{r}) \cdot \mathbf{n}_2(\mathbf{r}))\,. \end{aligned} \quad (7)$$

This result, together with the structure of the exact excess free energy functional of one-dimensional hard-rod mixtures, leads to the assumption that the excess free energy density $\Phi(\mathrm{r})$ can be approximated as a function of the six weighted densities only. This assumption guarantees to recover the exact low density limit of $\Phi(\mathrm{r})$. The expression for

the free energy density is obtained by an extrapolation of the known low-density result for $\Phi(\mathrm{r})$ to higher densities using thermodynamic arguments.

We consider the case of a homogeneous hard-sphere mixture, i.e. the density distributions $\rho_i(\mathbf{r}) \equiv \rho_i = N_i/V$ are constant. N_i is the number or spheres of species i in the volume V. The excess pressure p^{ex} of a fluid mixture can be obtained from the excess free energy density Φ via

$$\beta p^{\mathrm{ex}} = -\frac{\partial(V\Phi)}{\partial V} = -\Phi + \sum_{i=1}^{\nu} \frac{\partial \Phi}{\partial \rho_i}\rho_i = -\Phi + \sum_{\alpha} \frac{\partial \Phi}{\partial n_\alpha} n_\alpha \,. \tag{8}$$

Note that the vectorial weighted densities, which are formally included in the above sum, actually vanish in the uniform fluid. The ideal gas contribution to the pressure is $\beta p^{\mathrm{id}} = \sum_i \rho_i$, which in terms of the weighted densities reduces to $\beta p^{\mathrm{id}} = n_0$. Hence, according to thermodynamics (TD), the total pressure within FMT can be written as

$$\beta p_{\mathrm{TD}} = n_0 - \Phi + \sum_{\alpha} \frac{\partial \Phi}{\partial n_\alpha} n_\alpha \,. \tag{9}$$

On the other hand, there is an exact relation from scaled-particle (SP) theory (see [10] and references therein) between the chemical potential μ_i of species i for a very large sphere and the reversible work required for the creation of a cavity that can hold the large sphere of species i: in the limit $R_i \to \infty$ one obtains $\mu_i/V_i \to p_{\mathrm{SP}}$, where p_{SP} is the total pressure of the fluid mixture and $V_i = (4/3)\pi R_i^3$. In our context, this is equivalent to (cf. [10, 11])

$$\beta p_{\mathrm{SP}} = \frac{\partial \Phi}{\partial n_3} \,. \tag{10}$$

Obviously, we obtain a differential equation for Φ by equating the expressions for p_{TD} and p_{SP}. This equation was solved by Rosenfeld who used the ansatz

$$\Phi = f_1(n_3)n_0 + f_2(n_3)n_1 n_2 + f_3(n_3)\mathbf{n}_1 \cdot \mathbf{n}_2 + f_4(n_3)n_2^3 + f_5(n_3)n_2 \mathbf{n}_2 \cdot \mathbf{n}_2 \,, \tag{11}$$

with $f_1, \ldots, f_5$ being functions of the dimensionless weighted density n_3. The ansatz Eq. (11) combines all multiplicative combinations of the weighted densities which share the dimension of Φ, i.e. $(\mathrm{length})^{-3}$. There is a solution Φ_{RF} of the SPT differential equation. The integration constants can be fixed by the following additional requirements: (i) in the low-density limit, Eq. (7) is recovered, (ii) for the one-component uniform hard-sphere fluid the correct third virial coefficient is reproduced and (iii) the pair direct correlation function $c^{(2)}(r)$ is regular for $r \to 0$, which enforces the prefactor for the term $\propto n_2 \mathbf{n}_2 \cdot \mathbf{n}_2$. The result is

$$\Phi_{\mathrm{RF}} = -n_0 \ln(1-n_3) + \frac{n_1 n_2 - \mathbf{n}_1 \cdot \mathbf{n}_2}{1-n_3} + \frac{n_2^3 - 3n_2 \mathbf{n}_2 \cdot \mathbf{n}_2}{24\pi(1-n_3)^2} \,. \tag{12}$$

Rosenfeld's excess free energy gives a good account for many aspects of nonuniform hard-sphere fluids, pure [17, 18] or mixtures [19]. However, it does not predict freezing, which is actually observed for the pure hard-sphere fluid at a packing fraction $\eta \simeq 0.494$. This deficiency can be resolved empirically by modifying the third term in Eq. (12) [20, 21], or more systematically by the recipe of Tarazona [22] who introduced an

additional tensorial weighted density in the last term of $\Phi_{\rm RF}$. There remains another factor which limits the accuracy of $\Phi_{\rm RF}$, namely the equation of state obtained from Eq. (9) or, equivalently, Eq. (10). One finds the pressure

$$\beta p_{\rm PY} = \frac{n_0}{1-n_3} + \frac{n_1 n_2}{(1-n_3)^2} + \frac{n_2^3}{12\pi(1-n_3)^3}\,, \tag{13}$$

which is the compressibility expression from the solution of the PY integral equation [23]. The PY pressure is in good agreement with simulations for the pure hard-sphere fluid at low packing fractions but close to the freezing transition it overestimates the pressure by about 7%. This problem can be solved by incorporating more accurate equations of state within the context of Rosenfeld's FMT as an extrapolation from low to high densities [11, 12]. In the next section we introduce a new contribution along these lines.

3. The new functional

An empirical correction of the high-density behavior of the PY compressibility result has been given by Carnahan and Starling [24]. The CS equation of state has subsequently been generalized to hard-sphere mixtures resulting in the Boublík-Mansoori-Carnahan-Starling-Leland (BMCSL) pressure $p_{\rm BMCSL}$ [25, 26]. This equation of state can be written in terms of the weighted densities of a homogeneous hard-sphere mixture:

$$\beta p_{\rm BMCSL} = \frac{n_0}{1-n_3} + \frac{n_1 n_2}{(1-n_3)^2} + \frac{n_2^3\left(1-\frac{1}{3}n_3\right)}{12\pi(1-n_3)^3}\,. \tag{14}$$

Using this fact, $p_{\rm BMCSL}$ has been incorporated into FMT [11, 12]. This was achieved by solving the differential equation for the excess free energy Φ which is obtained by equating $p_{\rm BMCSL}$ and the thermodynamic expression $p_{\rm TD}$ as given in Eq. (9). Note that for the implementation of this approach a bulk fluid mixture is considered for which the vectorial weighted densities vanish. Hence, the solution of the resulting differential equation is obtained by using the dimensional ansatz Eq. (11) without the vectorial contributions. For this ansatz there is a unique solution if two additional requirements are made: (i) the result for Φ is compatible with the low-density limit Eq. (7) and (ii) for the pure hard-sphere fluid the third virial coefficient is recovered. Unlike in Rosenfeld's derivation of $\Phi_{\rm RF}$ the vectorial contributions have to be incorporated at a later stage. In analogy to $\Phi_{\rm RF}$ the substitutions $n_1 n_2 \to n_1 n_2 - \mathbf{n}_1 \cdot \mathbf{n}_2$ and $n_2^3 \to n_2^3 - 3 n_2 \mathbf{n}_2 \cdot \mathbf{n}_2$ are made in Φ. The resulting functional $\Phi_{\rm WB}$ is called the White-Bear version of FMT [11]. In virtue of these substitutions, $\Phi_{\rm WB}$ has the correct low-density limit Eq. (7) and the regularity of the pair direct correlation function for $r \to 0$ is guaranteed.

The White-Bear version of FMT has been shown to inherit all the good properties of Rosenfeld's FMT for the description of the hard-sphere fluid and improves the predictions of thermodynamic quantities due to the more accurate underlying equation of state. This becomes particularly apparent in the contact densities at a hard wall which are related to the pressure via a sum rule (for a comparison with simulation data

see, e.g. [27]). Furthermore, one finds that the prediction of the freezing transition of the pure hard-sphere system agrees very well with simulations [11]. A drawback of Φ_{WB} is, however, that the scaled particle relation Eq. (10) is violated, i.e. one finds that $\partial\Phi_{\mathrm{WB}}/\partial n_3 \neq p_{\mathrm{BMCSL}}$. This is of course not surprising as the equality $p_{\mathrm{TD}} = p_{\mathrm{SP}}$ unambiguously leads to Rosenfeld's Φ_{RF}, if we assume that the free energy density is a function of the weighted densities $n_0, \ldots, n_3$ and $\mathbf{n}_1$, and $\mathbf{n}_2$ alone. Despite this inconsistency of the White-Bear version, the quality of the resulting density distributions is high [13]. However, analytical results obtained from the free energy density Φ_{WB} within the context of morphological thermodynamics ([28] and references therein) are affected.

We conclude, that there is some room for improvement with respect to the self-consistency of the free energy density. The basis for this improvement is a new generalization of the CS pressure to mixtures of hard spheres which was recently suggested by the authors [14]. In terms of the weighted densities, the new equation of state reads

$$\beta p_{\mathrm{CSIII}} = \frac{n_0}{1-n_3} + \frac{n_1 n_2 \left(1 + \frac{1}{3}n_3^2\right)}{(1-n_3)^2} + \frac{n_2^3 \left(1 - \frac{2}{3}n_3 + \frac{1}{3}n_3^2\right)}{12\pi(1-n_3)^3}\,. \tag{15}$$

The index CSIII refers to a hierarchy of extensions introduced in Ref. [14], where we showed for binary and ternary hard-sphere mixtures that p_{CSIII} improves upon p_{BMCSL} compared to computer simulations. Even more interestingly for the present context, p_{CSIII} was constructed such that it is consistent with the scaled-particle relation Eq. (10) in the case of the one-component hard-sphere fluid. Note, that consistency for the general hard-sphere mixture within the framework of FMT would always result in the less accurate pressure p_{PY}.

By following the recipe for the derivation of the original White-Bear version [11, 12], described above, we calculate a new functional based on the pressure p_{CSIII}

$$\begin{aligned}\Phi_{\mathrm{WBII}} = & -n_0 \ln(1-n_3) + \left(1 + \tfrac{1}{9}n_3^2\phi_2(n_3)\right)\frac{n_1 n_2 - \mathbf{n}_1\cdot\mathbf{n}_2}{1-n_3} \\ & + \left(1 - \tfrac{4}{9}n_3\phi_3(n_3)\right)\frac{n_2^3 - 3n_2\mathbf{n}_2\cdot\mathbf{n}_2}{24\pi(1-n_3)^2}\end{aligned} \tag{16}$$

with

$$\begin{aligned}\phi_2(n_3) &= \left(6n_3 - 3n_3^2 + 6(1-n_3)\ln(1-n_3)\right)/n_3^3 = 1 + \tfrac{1}{2}n_3 + \mathcal{O}(n_3^2)\,, \\ \phi_3(n_3) &= \left(6n_3 - 9n_3^2 + 6n_3^3 + 6(1-n_3)^2\ln(1-n_3)\right)/(4n_3^3) = 1 - \tfrac{1}{8}n_3 + \mathcal{O}(n_3^2)\,.\end{aligned} \tag{17}$$

The new functional is an improvement of the White Bear version of FMT, as we shall show in Sec. 4. The index WBII is chosen to indicate that the new functional is Mark II of the White Bear functional.

For comparison we mention that in the above notation the original White-Bear functional Φ_{WB} is recovered with $\phi_2^{\mathrm{WB}}(n_3) \equiv 0$ and

$$\phi_3^{\mathrm{WB}}(n_3) = \left(9n_3^2 - 6n_3 - 6(1-n_3)^2\ln(1-n_3)\right)/(4n_3^3) = \tfrac{1}{2} + \tfrac{1}{8}n_3 + \mathcal{O}(n_3^2)\,. \tag{18}$$

We have compared predictions of our new version of FMT with corresponding results obtained by the original White-Bear version for a pure hard-sphere fluid and a

binary mixture close to a planar hard wall. We have found that the density distributions resulting from numerical minimization of the functional Eq. (1) with $\Phi_{\rm WB}$ or $\Phi_{\rm WBII}$, respectively, differ very little. For the pure hard-sphere fluid, this can be expected from the fact that the underlying bulk equation of state is the same for both versions of FMT and hence the contact densities at the wall have to be identical. Comparison with density distributions from Monte-Carlo simulations revealed that the very small deviations of the DFT results from the simulation data are clearly more significant than the mutual deviations between the two FMT versions. We conclude that the limitations of FMT-based density functionals cannot be considerable pushed forward by increasing the quality of the underlying bulk equation of state but are rather determined by the structure of FMT itself, i.e. the set of weight functions which are employed and hence the restriction to one-center convolutions. For a discussion of this topic see Ref. [29]. A slight improvement from the WBII version is indeed found for the description of the pair direct correlation function as can be inferred from comparison with simulation data (not shown).

We find the main benefit of the new functional $\Phi_{\rm WBII}$ in the context of morphological thermodynamics. Here, the self-consistency of $\Phi_{\rm WBII}$ on the level of the pressure, i.e. the equality of $p_{\rm TD}$ from Eq. (9) and $p_{\rm SP}$ from Eq. (10) in the case of the pure fluid, is crucial for the accuracy of analytical expressions obtained within the morphological theory. In the next section we give a brief introduction to the theory and show examples which illustrate the gain from the new functional $\Phi_{\rm WBII}$.

4. Morphological thermodynamics

The morphometric approach to the grand potential of a fluid around a complexly shaped object $\mathcal{B}$ (or a fluid inside a complexly shaped container) was inspired by the Hadwiger theorem [30] from integral geometry [31]. The theorem states that every motion-invariant, continuous and additive functional of the complexly shaped object $\mathcal{B}$ depends on the shape of $\mathcal{B}$ via only four geometric measures: the volume V, the surface area A, the integrated (over the surface area) mean and Gaussian curvature C and X, respectively. The latter are given as

$$C = \int\limits_{\partial\mathcal{B}} \mathrm{d}\mathbf{r}\, \frac{1}{2}\left(\frac{1}{R_1}+\frac{1}{R_2}\right), \quad X = \int\limits_{\partial\mathcal{B}} \mathrm{d}\mathbf{r}\, \frac{1}{R_1 R_2}\,. \tag{19}$$

Here R_1 and R_2 are the local principal radii of curvature on the surface of $\mathcal{B}$. Note that X is proportional to the Euler characteristic.

While the Hadwiger theorem is rigorous, the connection to physics is not obvious and cannot be proven rigorously. However, there is strong numerical evidence [32, 28, 27, 33, 34] that the solvation free energy of a convex body immersed in a solvent away from the critical point and away from wetting or drying transitions takes the form

$$\Delta\Omega = pV + \sigma A + \kappa C + \bar{\kappa} X\,. \tag{20}$$

where the conjugated quantities to the geometric measures of $\mathcal{B}$ are thermodynamic coefficients depending only on the temperature, the chemical potentials and the given interaction between $\mathcal{B}$ and the fluid, and among fluid particles, but not on the (complex) geometry of $\mathcal{B}$. The thermodynamic coefficients are p, the pressure, σ the planar wall surface tension, and κ and $\bar{\kappa}$ two bending rigidities.

Morphometry is obviously a very useful tool for the calculation of thermodynamic quantities in complex geometries as it allows one to calculate the shape-independent thermodynamic coefficients in simple geometry. The treatment of the actual complex geometry (or a set of different geometries) then only requires a straightforward calculation of the geometric measures. For instance, the morphometric approach has been applied successfully to the calculation of solvation free energies of a protein in various geometrical configurations [34] and to the thermodynamics of fluids in porous media [35].

The test geometry we choose here is the case where the particle $\mathcal{B}$ is a single hard sphere $\mathcal{S}$ of radius $R_{\rm s}$ immersed in a pure hard-sphere fluid with radius R and density ρ. The change in grand potential $\Delta\Omega$ due to the insertion of the sphere $\mathcal{S}$ is obtained by minimizing the density functional Eq. (1) with either $\Phi_{\rm WB}$ or $\Phi_{\rm WBII}$. From the equilibrium density profile $\rho_0(\mathbf{r})$ one can calculate $\Delta\Omega = \Omega[\rho_0(\mathbf{r})] - \Omega[\rho(\mathbf{r}) = \rho_{\rm bulk}]$. By repeating the calculation for different values of $R_{\rm s}$ the function $\Delta\Omega(R_{\rm s})$ is obtained numerically.

On the other hand, we have the morphometric prediction for $\Delta\Omega$, Eq. (20). In order to evaluate the morphometric solvation free energy it is most convenient to calculate the geometrical measures and the thermodynamic coefficients at the surface at which the density profile $\rho_0(\mathbf{r})$ jumps discontinuously to zero. This surface is parallel to the physical wall of $\mathcal{S}$ at normal distance R. Note that it is actually the parallel surface and not the physical surface that enters in the external potential $V_{\rm ext}(r)$ in Eq. (1) that $\mathcal{S}$ exerts on the fluid. In terms of the parallel surface, which is simply a sphere with radius $R_{\rm s} + R$, the morphometric form, Eq. (20), reads

$$\Delta\Omega(R_{\rm s}) = p\,\frac{4}{3}\pi(R_{\rm s}+R)^3 + \sigma\,4\pi(R_{\rm s}+R)^2 + \kappa\,4\pi(R_{\rm s}+R) + \bar{\kappa}\,4\pi\,. \tag{21}$$

The extraction of the thermodynamic coefficients p, σ, κ and $\bar{\kappa}$ from the values $\Delta\Omega(R_{\rm s})$ obtained by minimization of the density functional is therefore achieved by fitting Eq. (21) to the numerical DFT data for different values of $R_{\rm s}$. This fit was performed for the data from $\Phi_{\rm WB}$ and $\Phi_{\rm WBII}$ in the range $R_{\rm s} \in [2R, 10R]$ for various values of the packing fractions of the fluid. Indeed, we find the assumption made by Eq. (21) on the $R_{\rm s}$-dependence of $\Delta\Omega$ clearly confirmed and in accordance with previous results [28]. We shall come back to our results later on, referring to them as obtained via the "minimization route".

In virtue of its applicability to mixtures, FMT also provides analytical expressions for the thermodynamic coefficients p, σ, κ and $\bar{\kappa}$. For their derivation, we follow the ideas of Refs. [32, 36]. In Ref. [32] the curvature dependence of the excess surface grand potential and contact density of a hard-sphere fluid in contact with hard curved walls

was studied. The basic idea is to consider a binary bulk mixture consisting of a hard-sphere fluid with radius R and packing fraction η and a single sphere $\mathcal{S}$, which is the second component at infinite dilution, i.e. $\rho_{\rm s} \to 0$. $\Delta\Omega$ is then obtained as the excess chemical potential $\mu_{\rm s}^{\rm ex}$. $\mu_{\rm s}^{\rm ex}$ can be calculated as the derivative of the mixture excess free energy density with respect to $\rho_{\rm s}$. Using any of the above FMT expressions for the excess free energy Φ we find

$$\begin{aligned}\beta\Delta\Omega = \beta\mu_{\rm s}^{\rm ex} &= \lim_{\rho_{\rm s}\to 0}\frac{\partial\Phi}{\partial\rho_{\rm s}} \\ &= \frac{\partial\Phi}{\partial n_3}\,\frac{4}{3}\pi R_{\rm s}^3 + \frac{\partial\Phi}{\partial n_2}\,4\pi R_{\rm s}^2 + \frac{\partial\Phi}{\partial n_1}\,R_{\rm s} + \frac{\partial\Phi}{\partial n_0}\,.\end{aligned} \tag{22}$$

Note that all vectorial contributions in Φ vanish in the uniform bulk. Due to the limit $\rho_{\rm s} \to 0$ the partial derivatives of Φ are evaluated for the solvent only, i.e. a one-component uniform fluid with radius R and packing fraction η.

A comparison of Eqs. (21) and (22) allows to identify the thermodynamic coefficients, calculated for the parallel surface, with certain linear combinations of the partial derivatives of Φ. We find that

$$\begin{aligned}\beta p &= \frac{\partial\Phi}{\partial n_3}\,, \\ \beta\sigma &= \frac{\partial\Phi}{\partial n_2} - R\frac{\partial\Phi}{\partial n_3}\,, \\ \beta\kappa &= \frac{1}{4\pi}\frac{\partial\Phi}{\partial n_1} - 2R\frac{\partial\Phi}{\partial n_2} + R^2\frac{\partial\Phi}{\partial n_3}\,, \\ \beta\bar{\kappa} &= \frac{1}{4\pi}\frac{\partial\Phi}{\partial n_0} - \frac{R}{4\pi}\frac{\partial\Phi}{\partial n_1} + R^2\frac{\partial\Phi}{\partial n_2} - \frac{1}{3}R^3\frac{\partial\Phi}{\partial n_3}\,.\end{aligned} \tag{23}$$

The relation for the pressure is precisely the scaled particle relation, Eq. (10). In the following, we refer to the above analytical results for the thermodynamic coefficients as the outcome of the "bulk route".

We give the explicit results for the coefficients only for the case of the new excess free energy density $\Phi_{\rm WBII}$:

$$\begin{aligned}\frac{\beta p_{\rm WBII}}{\rho} &= \frac{1+\eta+\eta^2-\eta^3}{(1-\eta)^3}\,, \\ \frac{\beta\sigma_{\rm WBII}}{R\rho} &= -\frac{1+2\eta+8\eta^2-5\eta^3}{3(1-\eta)^3} - \frac{\ln(1-\eta)}{3\eta}\,, \\ \frac{\beta\kappa_{\rm WBII}}{R^2\rho} &= \frac{4-10\eta+20\eta^2-8\eta^3}{3(1-\eta)^3} + \frac{4\ln(1-\eta)}{3\eta}\,, \\ \frac{\beta\bar{\kappa}_{\rm WBII}}{R^3\rho} &= \frac{-4+11\eta-13\eta^2+4\eta^3}{3(1-\eta)^3} - \frac{4\ln(1-\eta)}{3\eta}\,.\end{aligned} \tag{24}$$

We emphasize that the pressure $p_{\rm WBII}$ is precisely the quasi-exact CS expression. This is not a trivial fact but rather a consequence of the construction of the novel mixture equation of state Eq. (15) [14]. In contrast, the original White-Bear version of FMT, which is based on a different mixture generalization of the CS pressure [25, 26]

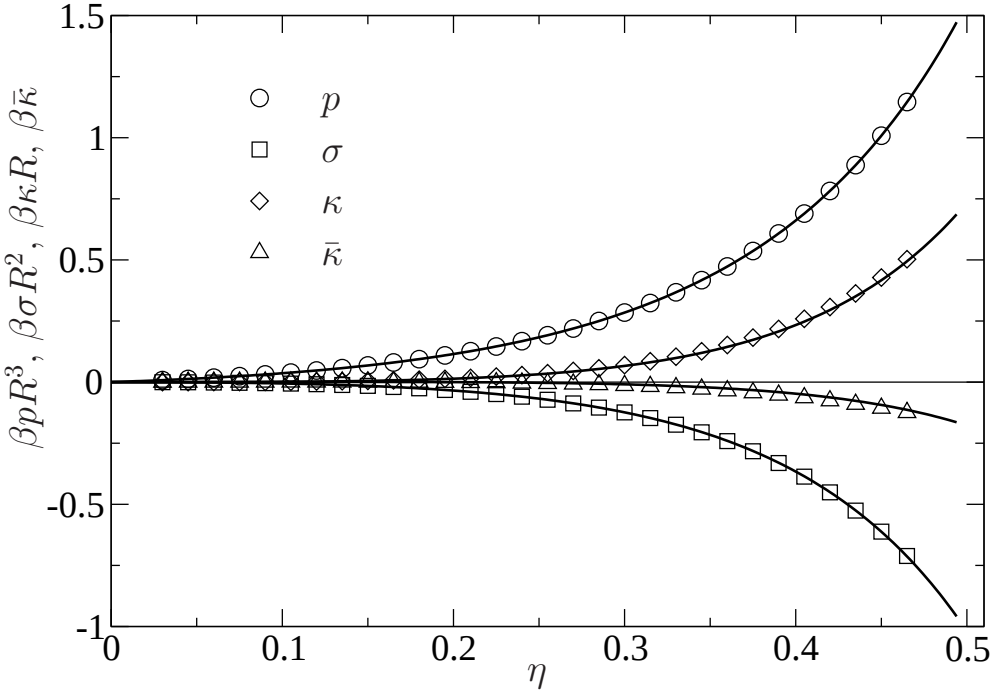

Figure 1. Results for the four thermodynamic coefficients p, σ, κ, and $\bar{\kappa}$ of the hard-sphere fluid are shown as obtained from the new excess free energy density $\Phi_{\rm WBII}$, Eq. (16). The analytical expressions given in Eqs. (24) are denoted by the lines, while the results from the minimization route are given by the symbols. η is the packing fraction. At $\eta \approx 0.494$ the hard-sphere fluid freezes.

does not possess this feature of self-consistency, i.e. the derivative of $\Phi_{\rm WB}$ with respect to n_3 does *not* yield exactly the CS pressure [11].

We now compare the results from the bulk and minimization routes as obtained for the different versions $\Phi_{\rm WB}$ and $\Phi_{\rm WBII}$ of FMT. In Fig. 1 we show our results for the thermodynamic coefficients calculated from the new functional $\Phi_{\rm WBII}$. The agreement for p is perfect by construction of the equation of state, Eq. (15), and very good for the surface tension σ. Note that from a comparison with simulation data $\sigma_{\rm WBII}$ was shown previously to be of high accuracy for intermediate and high packing fractions of the hard-sphere solvent. At low packing fractions, however, we found a small deviation from the exact low density limit of σ [14]. Only for the bending rigidities κ and $\bar{\kappa}$ a slight inconsistency between the bulk and the minimization route appears. However, this inconsistency remains below 1% at high values of η and we conjecture from the very good agreement of $\sigma_{\rm WBII}$ with simulation data that also $\kappa_{\rm WBII}$ and $\bar{\kappa}_{\rm WBII}$ deliver accurate expressions for the hard-sphere fluid thermodynamic coefficients. With Eqs. (24) we have obtained a set of analytical expressions for the thermodynamic coefficients that are more accurate than previous suggestions, namely the results calculated from the

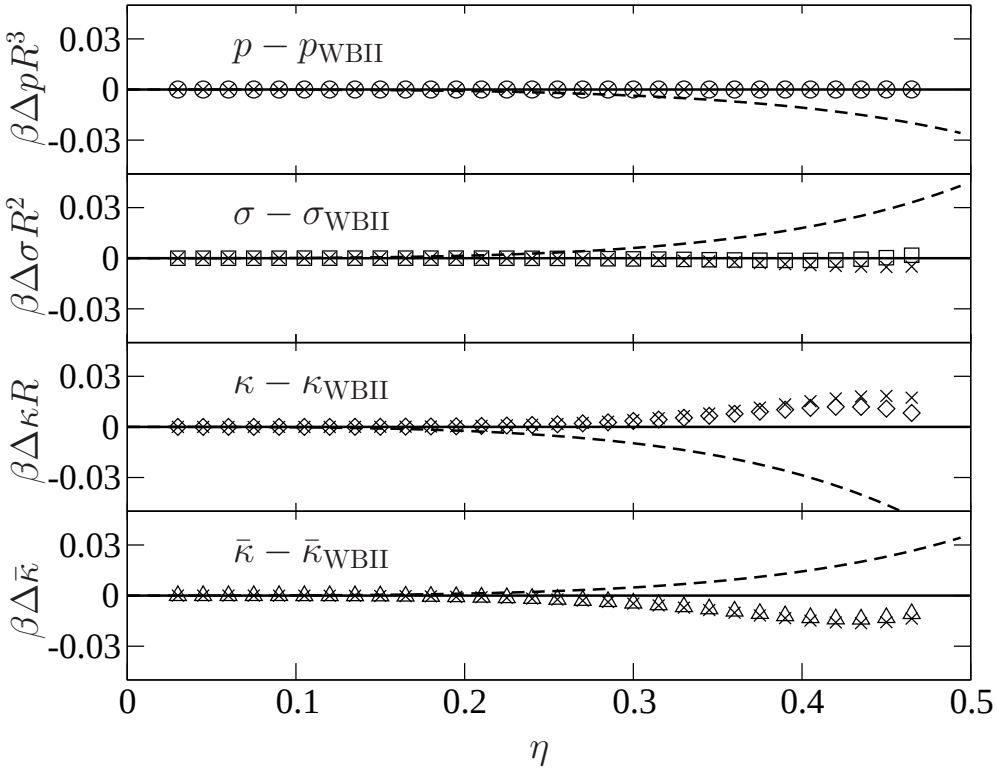

Figure 2. Various results for the four thermodynamic coefficients, p, σ, κ, and $\bar{\kappa}$. Shown are the differences of these coefficients obtained by various routes and theories to the analytical WBII results, Eqs. (24), cf. the lines in Fig. 1. The symbols (except the crosses) denote the WBII results from the minimization route. For comparison, we also show results from the original White-Bear version: those from the bulk route are plotted as dashed lines while the crosses denote the outcome of the minimization route.

original White-Bear version or those from Rosenfeld's DFT.

As an illustration, we plot in Fig. 2 the difference of various results for the four thermodynamic coefficients, p, σ, κ, and $\bar{\kappa}$ from the analytical expressions Eqs. (24) of the WBII version. Again, we find a high degree of self-consistency of the new functional Φ_{WBII} (symbols, except the crosses in Fig. 2). In contrast, the inconsistency of the original White-Bear version, which can be seen by the distance between the dashed line and the crosses in Fig. 2, is considerably larger and appears even for the pressure. The analytical expressions derived in the bulk route from Φ_{WB} are therefore of a lower quality than Eqs. (24), which manifests itself also in their poorer agreement with simulations [14]. The good agreement between the results from the minimization route for the two versions of FMT is a direct consequence of the good agreement in the corresponding density profiles. This observation can be rationalized by noting that the contact value of the density profile at a planar wall coincides for both version of FMT as a result of

the same bulk equation of state.

We do not include the results from Rosenfeld's functional $\Phi_{\rm RF}$ in Fig. 2 as this would require to extend the range of the vertical axis considerably and therefore obscure the examination of consistency of the White-Bear versions. When calculated from $\Phi_{\rm RF}$, however, the pressure follows the PY compressibility result which quantitatively differs from simulations so that the analytical expressions from the bulk route only yield a qualitative description of the thermodynamic coefficients. Surprisingly, the agreement between the bulk and the minimization route is comparable to that of $\Phi_{\rm WB}$ except for the pressure where $\Phi_{\rm RF}$ is consistent [37]. Intuitively, one might expect a better agreement for $\Phi_{\rm RF}$ than for $\Phi_{\rm WBII}$ because of the self-consistency on the level of the pressure. This interesting feature will be encountered again in the following where we consider the contact density at a curved hard wall.

The contact density of the hard-sphere fluid at a hard wall is connected to the normal derivative of the grand potential Ω [28]. The case of interest here is again a hard-sphere fluid (radius R, packing fraction η) around a sphere $\mathcal{S}$ with radius $R_{\rm s}$. We determine the grand potential from the density functional $\Omega[\rho_0(\mathbf{r})]$. The normal derivative of Ω reduces due to the symmetry to a derivative with respect to $R_{\rm s}$ at constant chemical potential, which is then calculated as

$$\frac{\partial\Omega}{\partial R_{\rm s}} = \int {\rm d}\mathbf{r}\, \frac{\delta\Omega[\rho_0(\mathbf{r})]}{\delta\rho} \frac{\partial\rho_0(\mathbf{r})}{\partial R_{\rm s}} + \int {\rm d}\mathbf{r}\, \rho_0(\mathbf{r}) \frac{\partial V_{\rm ext}(\mathbf{r})}{\partial R_{\rm s}}\,. \tag{25}$$

The first integral vanishes due to the equilibrium condition for $\rho_0(\mathbf{r})$, i.e. $\delta\Omega/\delta\rho = 0$. The derivative of the external potential gives rise to a δ-peak at the location of the parallel wall, and one finds [38]

$$\beta \frac{\partial\Omega}{\partial R_{\rm s}} = 4\pi (R_{\rm s} + R)^2 \rho_{\rm c} \tag{26}$$

where $\rho_{\rm c}$ is the contact value of the density of the fluid at the sphere $\mathcal{S}$. Using the morphometric form Eq. (21) for $\Delta\Omega$, the grand potential Ω of the fluid containing the sphere $\mathcal{S}$ is $\Omega(R_{\rm s}) = -pV_{\rm tot} + \Delta\Omega(R_{\rm s})$, where $V_{\rm tot}$ is the total volume of the system. In the thermodynamic limit $V_{\rm tot} \to \infty$. If the morphometric form is inserted into Eq. (26) one obtains the contact density $\rho_{\rm c}$

$$\rho_{\rm c} = \beta p + \frac{2\beta\sigma}{R_{\rm s} + R} + \frac{\beta\kappa}{(R_{\rm s} + R)^2}\,. \tag{27}$$

For $R_{\rm s} \to \infty$ the planar wall contact theorem $\rho_{\rm c} = \beta p$ is recovered and for finite values of $R_{\rm s}$ the contact density is lowered.

We show results for the contact density $\rho_{\rm c}$ of a hard-sphere fluid with packing fraction $\eta = 0.4$ as a function of the inverse of the radius $R_{\rm s}$ in Fig. 3. The symbols are the contact densities obtained from the density profiles which we calculated by minimizing numerically the functional Eq. (1). The lines in Fig. 3 show the morphometric prediction according to Eq. (27) with the analytical expressions for the thermodynamic coefficients from the different versions of FMT (cf. the bulk route above). The first observation we make is that the numerical results from $\Phi_{\rm WB}$ and $\Phi_{\rm WBII}$ are

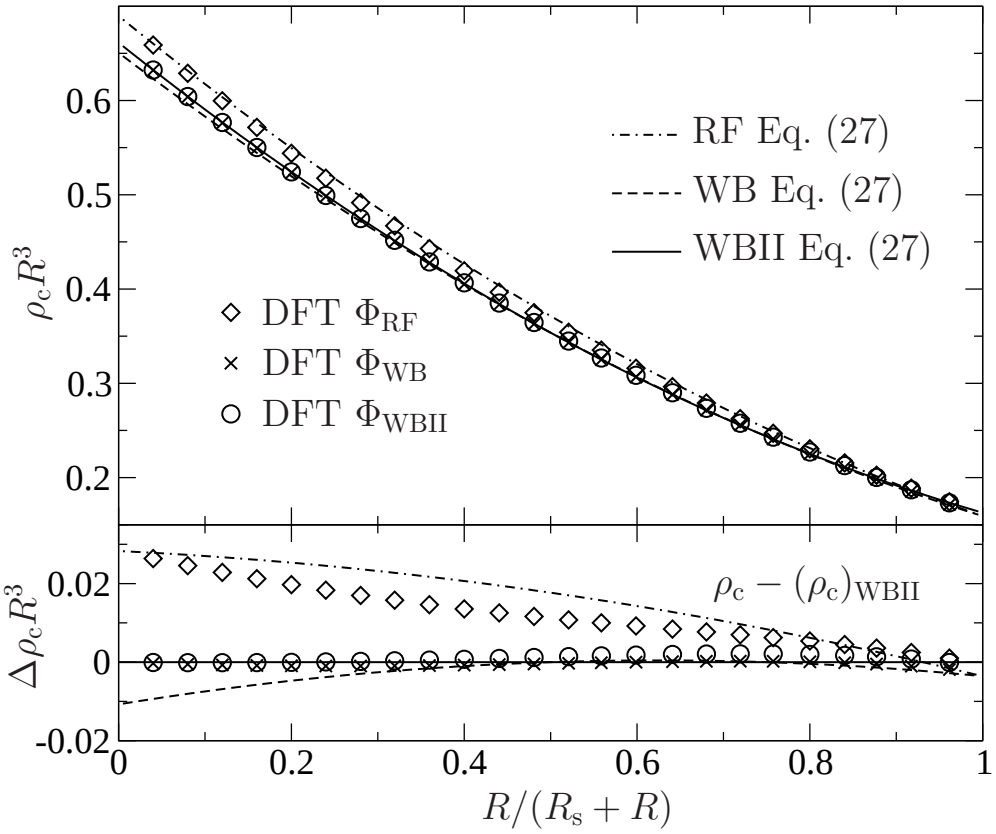

Figure 3. Contact value $\rho_{\rm c}$ of the density of a hard-sphere fluid (radius R, packing fraction $\eta = 0.4$) at a single sphere with radius $R_{\rm s}$. We show results obtained from the excess free energy densities $\Phi_{\rm RF}$, $\Phi_{\rm WB}$ and $\Phi_{\rm WBII}$, respectively. We compare results from the numerical minimization of the density functional (symbols), Eq. (1), with the morphometric prediction (lines) according to Eq. (27).

nearly indistinguishable and indeed in the planar wall limit, $R_{\rm s} \to \infty$, the data coincide by construction of the functionals. Taking this fact into account it is understandable that the results for $\rho_{\rm c}$ for finite values of $R_{\rm s}$ are very similar. The numerical data for $\Phi_{\rm RF}$ tends towards the PY pressure for $R_{\rm s} \to \infty$ which is known to overestimate the actual pressure in the hard-sphere fluid for sufficiently high values of η. In the limit $R_{\rm s} \to 0$ (point-like object) the data from the three versions of FMT coincide.

Comparing with the analytical prediction from morphometry, we find very good agreement between the results from $\Phi_{\rm WBII}$ over the whole interval of $R_{\rm s}$. Only for very small radii $R_{\rm s}$ a slight deviation is visible. Therefore, the new functional improves upon the results of the original White Bear version of FMT, which performs well at small radii, but produces a small error at large values of $R_{\rm s}$ due to the the inconsistency of $\Phi_{\rm WB}$ in the pressure.

As mentioned above for the thermodynamic coefficients, a moderate agreement in the case of Rosenfeld's FMT is also observed for the contact density. While the approach is consistent for large values of R_s by construction of the functional, in the range of smaller values of R_s a deviation is clearly visible. This behavior has been observed previously [32]. We find this fact remarkable because it shows that, from the point of view of self-consistency, the new hard-sphere mixture equation of state Eq. (15) is better suited for an implementation within FMT than the PY mixture equation of state Eq. (13) itself. This is even more surprising as the latter is characterized by full consistency for mixtures on the level of the pressure.

5. Conclusion

In this work, we have introduced a new density functional for hard-sphere mixtures which, in the spirit of the original White-Bear version, incorporates the quasi-exact CS equation of state within the framework of FMT. While the original White-Bear version is based on the well-known BMCSL equation of state, the White-Bear version Mark II, presented here, is derived from an improved mixture generalization of the CS equation of state recently introduced by us [14]. The new functional WBII, besides having all the good properties of the original White-Bear version, improves the level of self-consistency. The level of consistency of the WBII version for the pure hard-sphere fluid is examined in the context of morphological thermodynamics. Our study reveals that, beside the improved consistency of the pressure, also the consistency of the surface tension σ and the bending rigidities κ and $\bar{\kappa}$ is clearly improved. Supported by a previous comparison to simulation data for the surface tension [14] we can argue that the thermodynamic quantities derived from the new functional WBII are on a par with simulations.

We have presented evidence that in the case of the pure hard-sphere fluid the degree of self-consistency of the WBII version is even higher than that of Rosenfeld's original FMT. This is a remarkable finding as Rosenfeld's FMT is by construction fully (i.e. for an arbitrary mixture) consistent on the level of the pressure. Apparently, this fact does not translate into a high level of consistency for other thermodynamic quantities (such as surface tension and bending rigidities) of the pure fluid. We conclude that, in what concerns the pure hard-sphere fluid, the recent mixture generalization of the CS equation of state Eq. (15) is even better suited as a staring point for FMT than the PY compressibility mixture equation, underlying Rosenfeld's FMT. Note further that the PY mixture equation of state deviates significantly from simulations at sufficiently high densities.

In conclusion, with the WBII version we have constructed a new hard-sphere functional based on the CS pressure which improves upon the original White-Bear functional. Although the differences between the density profiles in simple geometries resulting from minimization of the functionals are small, the increased self-consistency of the WBII version proves crucial for analytical calculations within the context of morphological thermodynamics.

Our considerations are based on thermodynamic arguments and result in a change of the dependency of the free energy density Φ on the weighted density n_3. There are several other developments in FMT that were mainly concerned with improving the performance of FMT in highly confined geometries. These studies suggest to change the dependency of Φ on n_2 and $\mathbf{n}_2$ [20, 21] or to introduce new tensorial weighted densities [22]. It is worth pointing out that these improvements concerning the description of hard-sphere fluids in highly confined geometries are straightforwardly combined with the improvements on thermodynamics presented here.

References

[1] Evans R (1979) Adv. Phys. **28** 143.
[2] Evans R (1990) J. Phys.: Condens. Matter **2** 8989.
[3] Wu J (2006) AIChE J **52** 1169.
[4] Evans R (1992) in *Fundamentals of Inhomogeneous Fluids*, (ed. D. Henderson), 85 (Marcel Dekker, New York, NY)
[5] Hansen JP and McDonald IR, (1986) *Theory of simple liquids* (Academic Press, London).
[6] Rutgers MA, Dunsmuir JH, Xue J-Z, Russel WB, and Chaikin PM (1996) Phys. Rev. B **53** 5043.
[7] Roth R, Evans R, and Dietrich S (2000) Phys. Rev. E **62** 5360.
[8] Grodon C, Dijkstra M, Evans R, and Roth R (2004) J. Chem. Phys. **121** 7869.
[9] Grodon C, Dijkstra M, Evans R, and Roth R (2005) Mol. Phys. **103** 3009.
[10] Rosenfeld Y (1989) Phys. Rev. Lett. **63** 980.
[11] Roth R, Evans R, Lang A, and Kahl G (2002) J. Phys.: Condens. Matter **14** 12063.
[12] Yu Y-X and Wu J (2002) J. Chem. Phys. **117** 10156.
[13] Bryk P, Roth R, Schoen M, and Dietrich S (2003) Europhys. Lett. **63** 233.
[14] Hansen-Goos H and Roth R (2006) J. Chem. Phys. **124** 154506.
[15] Vanderlick TK, Davis HT, and Percus JK (1989) J. Chem. Phys. **91** 7136.
[16] Rosenfeld Y (1990) Phys. Rev. A **42** 5978.
[17] Kierlik E and Rosinberg ML (1990) Phys. Rev. A **42** 3382.
[18] Phan S, Kierlik E, Rosinberg ML, Bildstein B, and Kahl G (1993) Phys. Rev. E **48** 618.
[19] Roth R and Dietrich S (2000) Phys. Rev. E **62** 6926.
[20] Rosenfeld Y, Schmidt M, Löwen H, and Tarazona P (1996) J. Phys.: Condens. Matter **8** L577.
[21] Rosenfeld Y, Schmidt M, Löwen H, and Tarazona P (1997) Phys. Rev. E **55** 4245.
[22] Tarazona P (2000) Phys. Rev. Lett. **84** 694.
[23] Lebowitz JL (1964) Phys. Rev. **133** A895.
[24] Carnahan NF and Starling KE (1969) J. Chem. Phys. **51** 635.
[25] Boublík T (1970) J. Chem. Phys. **53** 471.
[26] Mansoori GA, Carnahan NF, Starling KE, and Leland TW (1971) J. Chem. Phys. **54** 1523.
[27] König P-M, Bryk P, Mecke K, and Roth R (2005) Europhys. Lett. **69** 832.
[28] König P-M, Roth R and Mecke KR (2004) Phys. Rev. Lett. **93** 160601.
[29] Cuesta JA, Martínez-Ratón Y, and Tarazona P (2002) J. Phys.: Condens. Matter **14** 11965.
[30] Hadwiger H (1957) *Vorlesungen über Inhalt, Oberfläche und Isoperimetrie* (Springer, Berlin, Germany).
[31] Mecke KR (1994) *Integralgeometrie in der Statistischen Physik* (Harri Deutsch, Frankfurt, Germany).
[32] Bryk P, Roth R, Mecke KR, and Dietrich S (2003) Phys. Rev. E **68** 031602.
[33] Roth R (2005) J. Phys.: Condens. Matter **17** S3463.
[34] Roth R, Harano Y, and Kinoshita M (2006) Phys. Rev. Lett., *accepted*.
[35] Mecke K and Arns CH (2005) J. Phys.: Condens. Matter **17** S503.

[36] Oversteegen SM and Roth R (2005) J. Chem. Phys. **122** 214502.
[37] König P-M (2005) doctoral thesis, ITAP, University of Stuttgart, Stuttgart.
[38] Henderson JR (1983) Mol. Phys. **50** 741.